Spin Transport of Excitons

J. R. Leonard,*,† Y. Y. Kuznetsova,† Sen Yang,† L. V. Butov,† T. Ostatnický,‡ A. Kavokin,‡,§ and A. C. Gossard‖

Department of Physics, University of California at San Diego, La Jolla, California 92093-0319, School of Physics and Astronomy, University of Southampton, SO17 1BJ, Southampton, United Kingdom, Dipartimento di Fisica, Universita' "Tor Vergata" via della Ricerca Scientifica, 00133 Rome, Italy, and Materials Department, University of California at Santa Barbara, Santa Barbara, California 93106-5050

ABSTRACT

We report on observation of the spin transport of spatially indirect excitons in GaAs/AlGaAs coupled quantum wells (CQW). Exciton spin transport over substantial distances, up to several micrometers in the present work, is achieved due to orders of magnitude enhancement of the exciton spin relaxation time in CQW with respect to conventional quantum wells.

Spin physics in semiconductors includes a number of interesting phenomena in electron transport, such as current-induced spin orientation (the spin Hall effect),[1−3] spin-induced contribution to the current,[4] spin injection,[5] and spin diffusion and drag.[6−11] Besides the fundamental spin physics, there is also considerable interest in developing semiconductor electronic devices based on the spin transport, which may offer advantages in dissipation, size, and speed over charge-based devices; see ref 12 and references therein.

Optical methods have been used as a tool for precise injection, probe, and control of electron spin via photon polarization in semiconductors. A major role in the optical properties of semiconductors near the fundamental absorption edge is played by excitons. The spin dynamics of excitons in GaAs single quantum wells (QW) was extensively studied in the past; see refs 13−15 and references therein. It was found that the spin relaxation time of excitons in single QW is of the order of a few tens of picoseconds. Because of the short spin relaxation time, no spin transport of excitons was observed until this work.

Here, we report on the observation of the spin transport of spatially indirect excitons in GaAs coupled quantum wells (CQW). The spin relaxation time of indirect excitons is orders of magnitude longer than one of regular direct excitons. In combination with a long lifetime of indirect excitons, this makes possible spin transport of indirect excitons over substantial distances.

The spin dynamics of excitons can be probed by the polarization resolved spectroscopy. In GaAs QW structures, the σ^+ (σ^-) polarized light propagating along the z axis creates a heavy hole exciton with the electron spin state $s_z = -1/2$ ($s_z = +1/2$) and hole spin state $m_h = +3/2$ ($m_h = -3/2$). In turn, heavy hole excitons with $S_z = +1$ (-1) emit σ^+ (σ^-) polarized light. Excitons with $S_z = \pm2$ are optically inactive. The polarization of the exciton emission $P = (I_+ - I_-)/(I_+ + I_-)$ is determined by the recombination and spin relaxation processes. For an optically active heavy hole exciton, an electron or hole spin-flip transforms the exciton to an optically inactive state (Figure 1a) causing no decay of emission polarization. The polarization of emission decays only when both the electron and hole flip their spins. This can occur in the two-step process due to the separate electron and hole spin flips and the single-step process due to the exciton spin flip.[13−15] The rate equations describing these processes[14,15] yield for the case when the splitting between $S_z = \pm1$ and ±2 states Δ is smaller than k_BT the polarization of the exciton emission $P = \tau_P/(\tau_P + \tau_r)$ and the relaxation time of the emission polarization $\tau_P^{-1} = 2(\tau_e + \tau_h)^{-1} + \tau_{ex}^{-1}$, where τ_{ex} time for exciton flipping between $S_z = \pm1$ states, τ_e and τ_h electron and hole spin flip times, and τ_r exciton recombination time.[30] The requirement $\Delta \ll k_BT$ is typically fulfilled for indirect excitons. Indeed, for regular direct excitons in single GaAs QW, $\Delta \lesssim 100~\mu\text{eV}$.[16] It is determined by the exchange interaction between the electron and hole in the exciton and scales $\propto \tau_r^{-1}$.[13−16] For indirect excitons in the studied CQW, τ_r is about thousand times larger than for direct excitons[17] and therefore $\Delta \lesssim 100$ neV $\ll k_BT$.

In GaAs single QW, τ_h and τ_{ex} are typically in the range of tens of picoseconds and are much shorter than τ_e so that
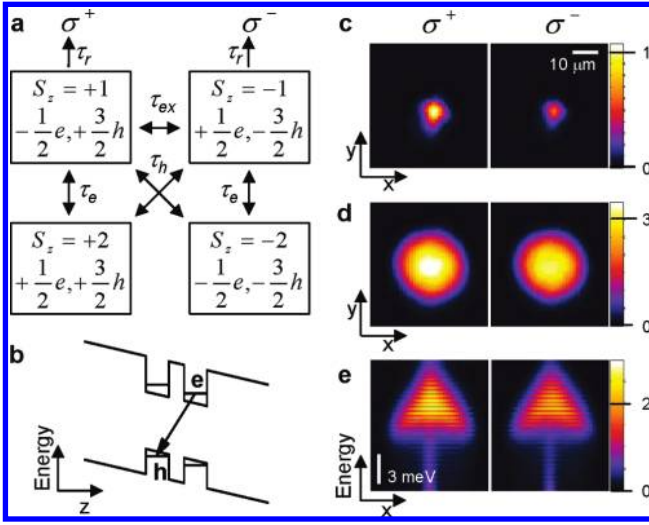
* To whom correspondence should be addressed, jleonard@physics.ucsd.edu.
† Department of Physics, University of California at San Diego, La Jolla.
‡ School of Physics and Astronomy, University of Southampton.
§ Dipartimento di Fisica, Universita' "Tor Vergata" via della Ricerca Scientifica.
‖ Materials Department, University of California at Santa Barbara.

Figure 1. Diagrams and PL images for excitons. (a) Exciton spin diagram. (b) Energy diagram of the CQW structure: e, electron; h, hole. x–y images of the PL intensity of indirect excitons in σ^+ and σ^- polarizations for (c) $P_{ex} = 4.7\ \mu$W and (d) $P_{ex} = 310\ \mu$W; $V_g = -1.1$ V, $E_{ex} = 1.582$ eV. (e) x-energy images of the PL intensity of indirect excitons in σ^+ and σ^- polarizations; $V_g = -1.1$ V, $E_{ex} = 1.572$ eV, $P_{ex} = 140\ \mu$W.

$\tau_P \approx \tau_{ex}$.[14,15,18] The short τ_{ex} results in fast depolarization of the exciton emission within tens of picoseconds in GaAs single QW[14,15] making exciton spin transport over substantial distances problematic. However, τ_{ex} is determined by the strength of the exchange interaction between the electron and hole. This gives an opportunity to control the depolarization rate by changing the electron–hole overlap, e.g., in QW structures with different QW widths or with an applied electric field.[14,15]

The electron–hole overlap is drastically reduced in CQW structures. An indirect exciton in CQW is composed from an electron and a hole confined in different wells (Figure 1b). As a result of the small electron–hole overlap, the recombination time τ_r of indirect excitons is orders of magnitude longer than that of regular direct excitons and is typically in the range between tens of nanoseconds to tens of microseconds.[19] Long lifetimes of indirect excitons make possible their transport over large distances.[20–23] However, the ability to travel is required yet insufficient condition for spin transport. Exciton spin transport over substantial distances also requires a long spin relaxation time. The small electron–hole overlap for indirect excitons should also result to a large $\tau_{ex} \propto \tau_r^2$ and in turn τ_P, thus making possible exciton spin transport over substantial distances.

We probed exciton spin transport in a GaAs/AlGaAs CQW structure with two 8 nm GaAs QWs separated by a 4 nm Al$_{0.33}$Ga$_{0.67}$As barrier (see sample details in ref 17 where the same sample was studied). The electric field across the sample was controlled by an applied gate voltage V_g. The excitons were photoexcited by a continuous wave Ti:sapphire laser tuned to the direct exciton energy, $E_{ex} = 1.572$ eV, and focused to a spot of $\sim$5 μm in diameter. The spatial profile of the laser excitation spot was deduced from the profile of the bulk GaAs emission from the excitation spot. The excitation was circularly polarized (σ^+).
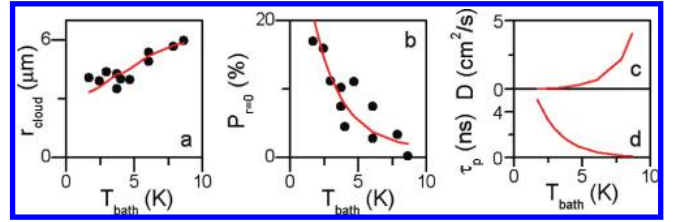
Figure 2. Temperature dependence. Experimental (points) and simulated (curves) (a) exciton cloud radius and (b) degree of circular polarization at the exciton cloud center as a function of temperature. (c, d) Fit parameters, diffusion coefficient D and polarization relaxation time τ_P as a function of temperature.

The emission images in σ^+ and σ^- polarizations were taken by a CCD camera with an interference filter 800 ± 5 nm, which covers the spectral range of the indirect excitons. The spatial resolution was 1.4 μm. The spectra were measured using a spectrometer with a resolution of 0.3 meV. The characteristic x-energy spectra and x–y images are shown in Figure 1c–e. The exciton density n was estimated from the energy shift as in ref 23. For recent discussions of the exciton–exciton interaction strength and the exciton density estimation see refs 24 and 25. We note that the results on exciton spin transport reported here are practically insensitive to the interaction strength.

Phenomenological Model for Exciton Spin Transport. Rate equations combining the exciton spin relaxation equations[14,15] with the drift-diffusion equation[23] yield

$$2\frac{\partial n_{\pm 1}}{\partial t} = 2\nabla[D\nabla n_{\pm 1} + 2\mu n_{\pm 1}\nabla(u_0 n_b)] - \frac{1}{\tau_r}n_{\pm 1} -$$
$$\frac{1}{2\tau_P}(n_{\pm 1} - n_{\mp 1}) + \Lambda\delta_{+,\pm} \quad (1)$$

where D is the exciton diffusion coefficient, $\mu \approx D/k_B T$ mobility, u_0 interaction energy estimated by $u_0 = 4\pi^2 d/\varepsilon$, $n_b = n_{+1} + n_{-1}$, and Λ generation rate of $+1$ excitons.[30] Both bright and dark exciton states are accounted for in eq 1; however the fast hole spin flip process allowed the simplification of the set of four coupled equations for four exciton spin species to the form of eq 1, which contain only two bright exciton states $n_{\pm 1}$.[30] $n_{+1}(r)$, $n_{-1}(r)$, and $P(r)$ were calculated using eq 1 and compared to the experimental data.

Temperature Dependence. Increasing the temperature leads to the increase of the exciton cloud radius r_{cloud} and decrease of the circular polarization of exciton emission at the excitation spot center $P_{r=0}$ (Figure 2a,b). The exciton cloud expansion $r_{cloud} \sim (D\tau_r)^{1/2}$ is determined by the exciton diffusion coefficient D. The circular polarization of exciton emission $P = \tau_P/(\tau_P + \tau_r)$ is determined by the depolarization time of the emission τ_P. Therefore, the measurements of r_{cloud}, P, and τ_r allow estimating D and τ_P. D and τ_P were extracted from the measured r_{cloud}, $P_{r=0}$, and τ_r[17] via numerical simulations using eq 1. The obtained temperature dependencies for D and τ_P are plotted in Figure 2c,d. The data show that (i) the depolarization time of the emission of indirect excitons reaches several nanoseconds, orders of magnitude longer than that of direct excitons in single QW,[14,15] (ii) the
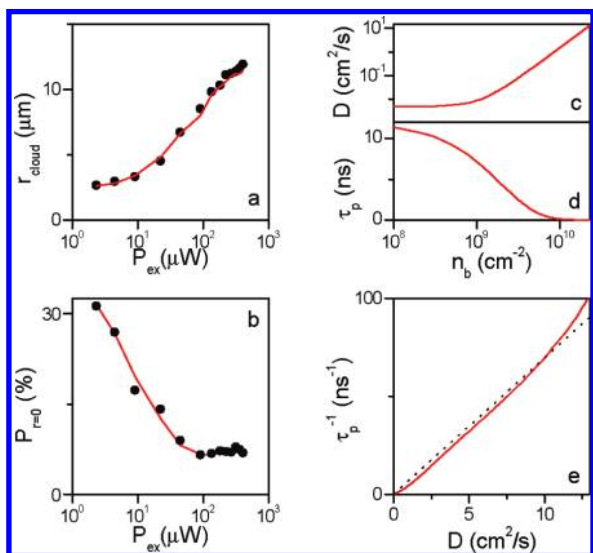
Figure 3. Density dependence. Experimental (points) and simulated (curves) (a) exciton cloud radius and (b) degree of circular polarization at the exciton cloud center as a function of excitation density. (c, d) Fit parameters, diffusion coefficient D and polarization relaxation time τ_P as a function of $n_b = n_{+1} + n_{-1}$. (e) $1/\tau_P$ vs D.

polarization rapidly decreases with increasing temperature, and (iii) the decrease of polarization is correlated with the increase of the diffusion coefficient.

Density Dependence. Increasing the density leads to the increase of r_{cloud} and decrease of $P_{r=0}$ (Figure 3a,b). At low densities, r_{cloud} is essentially equal to the excitation spot radius. Similar to the case of temperature dependence, these measurements of r_{cloud} and P allow estimating D and τ_P as a function of density. The measured r_{cloud} and $P_{r=0}$ were simulated using eq 1 with D and τ_P as fitting parameters. The obtained density dependencies for D and τ_P are plotted in Figure 3c,d. The polarization degree of the exciton emission and the polarization relaxation time reduce with increasing density (Figure 3b,d). Similar to the case of temperature dependence, the decrease of polarization is correlated with the increase of the diffusion coefficient. Figure 3e shows τ_P^{-1} vs D for the data in Figure 3c,d.

Spatial Dependence: Exciton Spin Transport. The polarization at half-width at half-maximum (HWHM) of the exciton cloud P_{HWHM} is observed up to several micrometers away from the origin (Figure 4a). This gives a rough estimate for the length scale of exciton spin transport. Figure 4a,b also shows P_{HWHM} and the spatially average polarization (P) calculated using eq 1 with D and τ_p in Figure 3c,d obtained from fitting r_{cloud} and $P_{r=0}$ data in Figure 3a,b.

Essential characteristics of the exciton spin transport are presented in Figure 4c−e. Figure 4c shows the measured PL in σ^+ and σ^- polarization as a function of the distance from the excitation spot center r. Figure 4d shows the corresponding $n_{+1}(r)$ and $n_{-1}(r)$ calculated using eq 1 with D and τ_P in Figure 3c,d. The polarization profiles are wider than the excitation spot that directly shows exciton spin transport (Figure 4e). The measured and calculated data on exciton spin transport are in agreement (Figure 4).
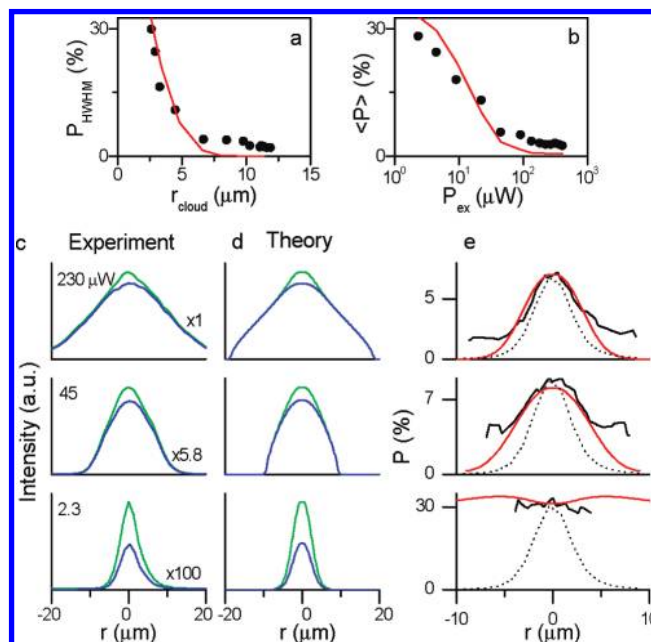
Figure 4. Exciton spin transport. (a) Experimental (points) and simulated (curve) polarization at HWHM of the exciton cloud P_{HWHM} as a function of r_{cloud}. (b) Experimental (points) and simulated (curve) spatially average polarization (P) as a function of excitation density. (c) PL intensity of indirect excitons in σ^+ and σ^- polarizations (green and blue curves) as a function of r for $P_{ex} = 2.3$, 45, and 230 μW with estimated densities at $r = 0$ of 9×10^8, 2×10^{10}, and 4×10^{10} cm^{-2}, respectively. (d) Simulated $n_{+1}(r)$ and $n_{-1}(r)$ for the same exciton densities as in (c). (e) Experimental (black curves) and simulated (red curves) PL polarization as a function of r for the same exciton densities as in (c, d). The profile of the bulk emission, which presents the excitation profile, is shown by dotted line. $T_{bath} = 1.7$ K. The simulations in (a, b, d, e) use $D(n)$ and $\tau_P(n)$ in Figure 3c,d.

The parameters used in the calculations of exciton spin transport D, τ_P, and τ_r were obtained from other experiments, different from exciton spin transport experiments: D, from exciton transport; τ_P, from emission polarization at the excitation spot center, and τ_r, from PL kinetics. The agreement between the calculated and measured data (Figure 4) indicates that the major characteristics of exciton spin transport are determined by D, τ_P, and τ_r. The following assumptions were made in the model: (i) splitting between optically active and dark exciton states is small $\Delta \ll k_B T$, (ii) hole spin flip is fast $\tau_h \ll \tau_e$, τ_{ex} and $\nabla[D\nabla\bar{n} + \mu\bar{n}\nabla(u_0 n_{total})] \ll \bar{n}/(2\tau_h)$, and (iii) conversion of the direct excitons into indirect excitons is fast $\tau_c \ll \tau_{P,d}$; see ref 30. The agreement between the experiment and the model (see Figure 4) indicates that these assumptions are justified and the model accurately describes exciton spin transport.

Discussion. Spin transport requires the ability of particles to travel maintaining spin polarization. This, in turn, requires large τ_r, D, and τ_P. Large τ_r and D are required to achieve exciton transport over substantial distances since the exciton diffusion length is determined by $(D\tau_r)^{1/2}$, while large τ_P is required for maintaining spin polarization during the transport. Large τ_r is characteristic for indirect excitons for which it is orders of magnitude larger than that for regular direct excitons. Large D is achieved with increasing exciton density (Figure

3a,c). This behavior is consistent with the localization−delocalization transition: Excitons are localized at low densities due to disorder and delocalized at high densities when the disorder is screened by repulsively interacting indirect excitons.[23,25] Localized excitons do not travel beyond the excitation spot while delocalized excitons spread over the distance $\sim (D\tau_r)^{1/2}$. This accounts for the density dependence of r_{cloud} and D (Figure 3a,c). r_{cloud} and D also increase with temperature (Figure 2a,c), because of thermal activation of indirect excitons over maxima of the disorder potential.

For indirect excitons with a small electron−hole overlap $\tau_{ex} \propto \tau_r^2$ is large, $\tau_{ex} \gg \tau_e$, and $\tau_P \approx \tau_e/2$ so that the polarization relaxation is governed by the electron spin relaxation and, therefore, can be long. Indeed, τ_P for indirect excitons at low temperatures and low densities reaches 10 ns (Figures 2d and 3d), much longer than τ_P for regular excitons, which is in the range of tens of picoseconds.[14,15] This orders of magnitude enhancement of the spin relaxation time for indirect excitons is achieved due to a small electron−hole overlap.

However, P and τ_P for indirect excitons drop with increasing temperature and density (Figures 2 and 3). For qualitative understanding of this behavior, we compare the variations of the polarization relaxation time and diffusion coefficient. Figures 2c,d and 3c,d show that τ_P^{-1} increases with D when the temperature or density is varied. This behavior complies with the D'yakonov-Perel' (DP) spin relaxation mechanism[26] for which the spin relaxation time $\tau_{e,ex}^{-1} = \langle \Omega_{e,ex}^2 \tau \rangle$, where $\Omega_{e,ex}$ is the frequency of spin precession caused by the energy splitting between different spin states, $\tau \approx m_{ex} D/(k_B T)$ momentum scattering time, and m_{ex} exciton mass.

Parts a and e of Figure 4 show that the length scale for exciton spin transport reaches several micrometers. It is large enough (i) for studying exciton spin transport by optical experiments, (ii) for studying spin-polarized exciton gases in microscopic patterned devices, e.g., in in-plane lattices,[25] in which the period can be below a micrometer, and (iii) for the development of spin-optoelectronic devices where *spin* fluxes of excitons can be controlled in analogy to the control of fluxes of unpolarized excitons in ref 27 (the distance between source and drain in the excitonic transistor in ref 27 was 3 μm; however, it is expected that the dimensions can be reduced below 1 μm by using e-beam lithography). The length scale for exciton spin transport exceeds the length scale for electron spin transport in metals where it is typically below 1 μm.[28]

Estimation of Spin Splitting. The measured dependence $\tau_P^{-1}(D)$ can be used to estimate the spin splitting. For the splitting of electron states caused by the Dresselhaus mechanism,[29] which is a likely scenario, $\Omega_e = 2\beta k/\hbar$ where k is the electron wave-vector. For the average thermal k of an electron in an exciton $k_T = (2m_{ex}k_B T/\hbar^2)^{1/2}m_e/m_{ex}$, one obtains $\tau_P^{-1} = 2\tau_e^{-1} = 16\beta^2 m_e^2 D/\hbar^4$ (m_e is electron mass) and the measured $\tau_P^{-1}(D)$ (Figure 3c) leads to the estimate of the spin splitting constant $\beta \approx 25$ meV Å.

The value of β for $\langle 001 \rangle$ oriented QW can be also roughly estimated as $\beta = \gamma_c \langle k_z^2 \rangle \approx \gamma_c(\pi/a)^2$, where a is the extension of the electron wave function in the QW and $\gamma_c \approx 27.5$ eV Å^3 is the bulk GaAs Dresselhaus constant.[29] For the studied CQW structure with a confining potential of 8 nm width and 260 meV depth, we obtain $\beta \approx 20$ meVÅ, in agreement with the experiment.

In conclusion, the spin transport of indirect excitons has been observed. It originates from a long spin relaxation time and long lifetime of indirect excitons. The phenomenological model for exciton spin transport is in agreement with the experiment.

Supporting Information Available: Details of exciton spin dynamics, the phenomenological model for exciton spin transport, and direct to indirect exciton conversion. This material is available free of charge via the Internet at http://pubs.acs.org.

References

(1) D'yakonov, M. I.; Perel', V. I. Current-induced spin orientation of electrons in semiconductors. *Phys. Lett. A* **1971**, *35*, 459.
(2) Hirsch, J. E. Spin Hall Effect. *Phys. Rev. Lett.* **1999**, *83*, 1834.
(3) Sih, V.; Myers, R. C.; Kato, Y. K.; Lau, W. H.; Gossard, A. C.; Awschalom, D. D. Spatial imaging of the spin Hall effect and current-induced polarization in two-dimensional electron gases. *Nat. Phys.* **2005**, *1*, 31.
(4) D'yakonov, M. I.; Perel', V. I. Possibility of orienting electron spins with current. *Zh. Eksp. Teor. Fiz. Pis'ma Red.* **1971**, *13*, 657. *Sov. Phys. JETP Lett.* **1971**, *13*, 467.
(5) Aronov, A. G.; Pikus, G. E. Spin injection into semiconductors. *Fiz. Tekh. Poluprovodn.* **1976**, *10*, 1177. *Sov. Phys. Semicond.* **1976**, *10*, 698.
(6) Dzhioev, R. I.; Zakharchenya, B. P.; Korenev, V. L.; Stepanova, M. N. Spin diffusion of optically oriented electrons and photon entrainment in n-gallium arsenide. *Fiz. Tverd. Tela* **1997**, *39*, 1975. *Phys. Solid State* **1997**, *39*, 1765.
(7) Kikkawa, J. M.; Awschalom, D. D. Lateral drag of spin coherence in gallium arsenide. *Nature* **1999**, *397*, 139.
(8) D'Amico, I.; Vignale, G. Spin diffusion in doped semiconductors: The role of Coulomb interactions. *Europhys. Lett.* **2001**, *55*, 566.
(9) Weber, C. P.; Gedik, N.; Moore, J. E.; Orenstein, J.; Stephens, J.; Awschalom, D. D. Observation of spin Coulomb drag in a two-dimensional electron gas. *Nature* **2005**, *437*, 1330.
(10) Carter, S. G.; Chen, Z.; Cundiff, S. T. Optical Measurement and Control of Spin Diffusion in n-Doped GaAs Quantum Wells. *Phys. Rev. Lett.* **2006**, *97*, 136602.
(11) Appelbaum, I.; Huang, Biqin; Monsma, D. J. Electronic measurement and control of spin transport in silicon. *Nature* **2007**, *447*, 295.
(12) Awschalom, D. D.; Flattté, M. E. Challenges for semiconductor spintronics. *Nat. Phys.* **2007**, *3*, 153.
(13) Andreani, L. C.; Bassani, F. Exchange interaction and polariton effects in quantum-well excitons. *Phys. Rev. B* **1990**, *41*, 7536.
(14) Maialle, M. Z.; de Andrada e Silva, E. A.; Sham, L. J. Exciton spin dynamics in quantum wells. *Phys. Rev. B* **1993**, *47*, 15776.
(15) Vinattieri, A.; Shah, Jagdeep; Damen, T. C.; Kim, D. S.; Pfeiffer, L. N.; Maialle, M. Z.; Sham, L. J. Exciton dynamics in GaAs quantum wells under resonant excitation. *Phys. Rev. B* **1994**, *50*, 10868.
(16) See, e.g.: Ivchenko, E. L. *Optical spectroscopy of semiconductor nanostructures*; Alpha Science International: Harrow, U.K., 2005.
(17) Butov, L. V.; Imamoglu, A.; Mintsev, A. V.; Campman, K. L.; Gossard, A. C. Photoluminescence kinetics of indirect excitons in GaAs/Al$_x$Ga$_{1-x}$As coupled quantum wells. *Phys. Rev. B* **1999**, *59*, 1625.
(18) Uenoyama, T.; Sham, L. J. Carrier relaxation and luminescence polarization in quantum wells. *Phys. Rev. B* **1990**, *42*, 7114.
(19) Alexandrou, A.; Kash, J. A.; Mendez, E. E.; Zachau, M.; Hong, J. M.; Fukuzawa, T.; Hase, Y. Electric-field effects on exciton lifetimes in

symmetric coupled GaAs/Al$_{0.3}$Ga$_{0.7}$As double quantum wells. *Phys. Rev. B* **1990**, *42*, 9225.

(20) Hagn, M.; Zrenner, A.; Böhm, G.; Weimann, G. Electric-field-induced exciton transport in coupled quantum well structures. *Appl. Phys. Lett.* **1995**, *67*, 232.

(21) Larionov, A. V.; Timofeev, V. B.; Hvam, J.; Soerensen, K. Interwell excitons in GaAs/AlGaAs double quantum wells and their collective properties. *Sov. Phys. JETP* **2000**, *90*, 1093.

(22) Gärtner, A.; Holleithner, A. W.; Kotthaus, J. P.; Schul, D. Drift mobility of long-living excitons in coupled GaAs quantum wells. *Appl. Phys. Lett.* **2006**, *89*, 052108.

(23) Ivanov, A. L.; Smallwood, L. E.; Hammack, A. T.; Yang, Sen; Butov, L. V.; Gossard, A. C. Origin of the inner ring in photoluminescence patterns of quantum well excitons. *Europhys. Lett.* **2006**, *73*, 920.

(24) Schindler, C.; Zimmermann, R. Analysis of the exciton-exciton interaction in semiconductor quantum wells. *Phys. Rev. B* **2008**, *78*, 045313.

(25) Remeika, M.; Graves, J. C.; Hammack, A. T.; Meyertholen, A. D.; Fogler, M. M.; Butov, L. V.; Hanson, M.; Gossard, A. C. Localization-Delocalization Transition of Indirect Excitons in Lateral Electrostatic Lattices. *Phys. Rev. Lett.* **2009**, *102*, 186803.

(26) D'yakonov, M. I.; Perel', V. I. Spin orientation of electrons associated with the interband absorption of light in semiconductors. *Zh. Eksp. Teor. Fiz.* **1971**, *60*, 1954. *Sov. Phys. JETP* **1971**, *33*, 1053.

(27) High, A. A.; Novitskaya, E. E.; Butov, L. V.; Hanson, M.; Gossard, A. C. Control of Exciton Fluxes in an Excitonic Integrated Circuit. *Science* **2008**, *321*, 229.

(28) Bass, J.; Pratt, W. P., Jr. Spin-diffusion lengths in metals and alloys, and spin-flipping at metal/metal interfaces: an experimentalist's critical review. *J. Phys.: Condens. Matter* **2007**, *19*, 183201.

(29) D'yakonov, M. I.; Kachorovskii, V. Yu. Spin relaxation of two-dimensional electrons in noncentrosymmetric semiconductors. *Fiz. Tekh. Poluprovodn.* **1986**, *20*, 178. *Sov. Phys. Semicond.* **1986**, *20*, 110.

(30) Supplementary online materials.

NL9024227